

SAK-HV Triggered a Short-period Lipid-lowering Biotherapy Based on the Energy Model of Liver Proliferation via a Novel Pathway

Chao Zhang, Zhiguang Huang, Haoran Jing, Wenliang Fu, Min Yuan, Wenrong Xia,
Ling Cai, Xiangdong Gan, Yao Chen, Minji Zou, Minhui Long, Jiayi Wang,
Min Wang*, and Donggang Xu*

From the Laboratory of Genome Engineering, Beijing Institute of Basic Medical
Sciences, Beijing, PR China.

Table of Contents

Supplementary figures and figure legends	2
Figure S1.....	2
Figure S2.....	3
Figure S3.....	4
Figure S4.....	5
Figure S5.....	6
Figure S6.....	7
Figure S7.....	8
Figure S8.....	9
Figure S9.....	10
Supplementary Tables	11
Table S1	11
Table S2	13
Table S3	14
Table S4	17
Table S5	19
Table S6	20
Table S7	23
Table S8	25
Table S9	26
Supplementary methods	28
Animal experiments design.....	28
Supplementary information.....	31
Introduction about SAK-HV.	31

Supplementary figures and figure legends

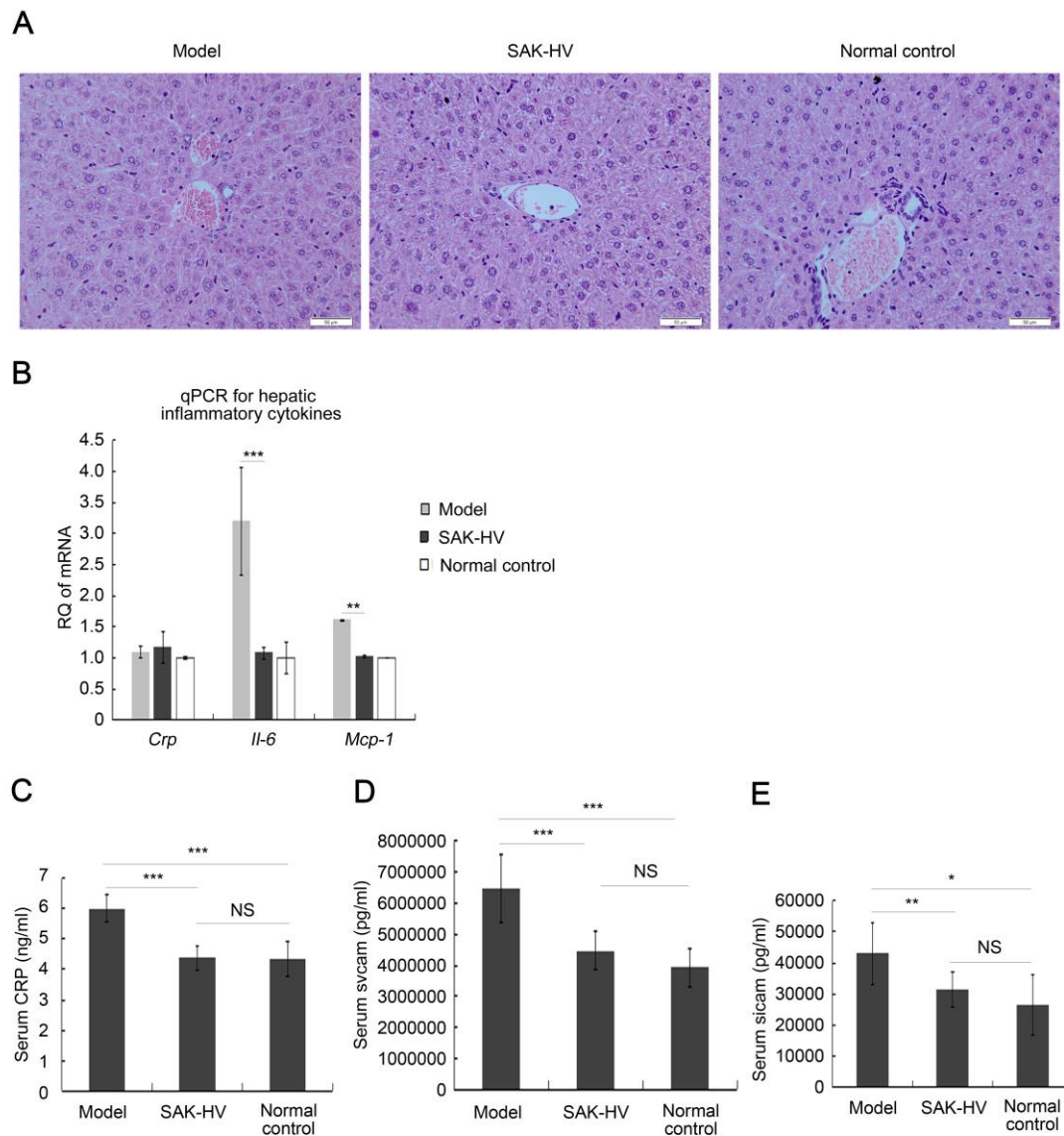


Figure S1. The histological and inflammatory assessment of the liver. (A) Representative images of liver sections stained with hematoxylin and eosin indicated that the morphology of liver was mildly improved without necrosis in the SAK-HV (0.125 mg/kg) group compared with that of model group (n=3). (B) The expression of inflammatory cytokines in liver after SAK-HV treatment (0.125 mg/kg) was decreased to the level similar to that of the normal group (n=8). (C-E) The serum levels of inflammatory cytokines after SAK-HV treatment (0.125 mg/kg) were decreased to the level similar to that of the normal group (n=8). Abbreviation: *Crp*, C-reaction protein; *Mcp1*, monocyte chemotactic protein 1; NS, no significance. * $P < 0.05$; ** $P < 0.01$; *** $P < 0.001$.

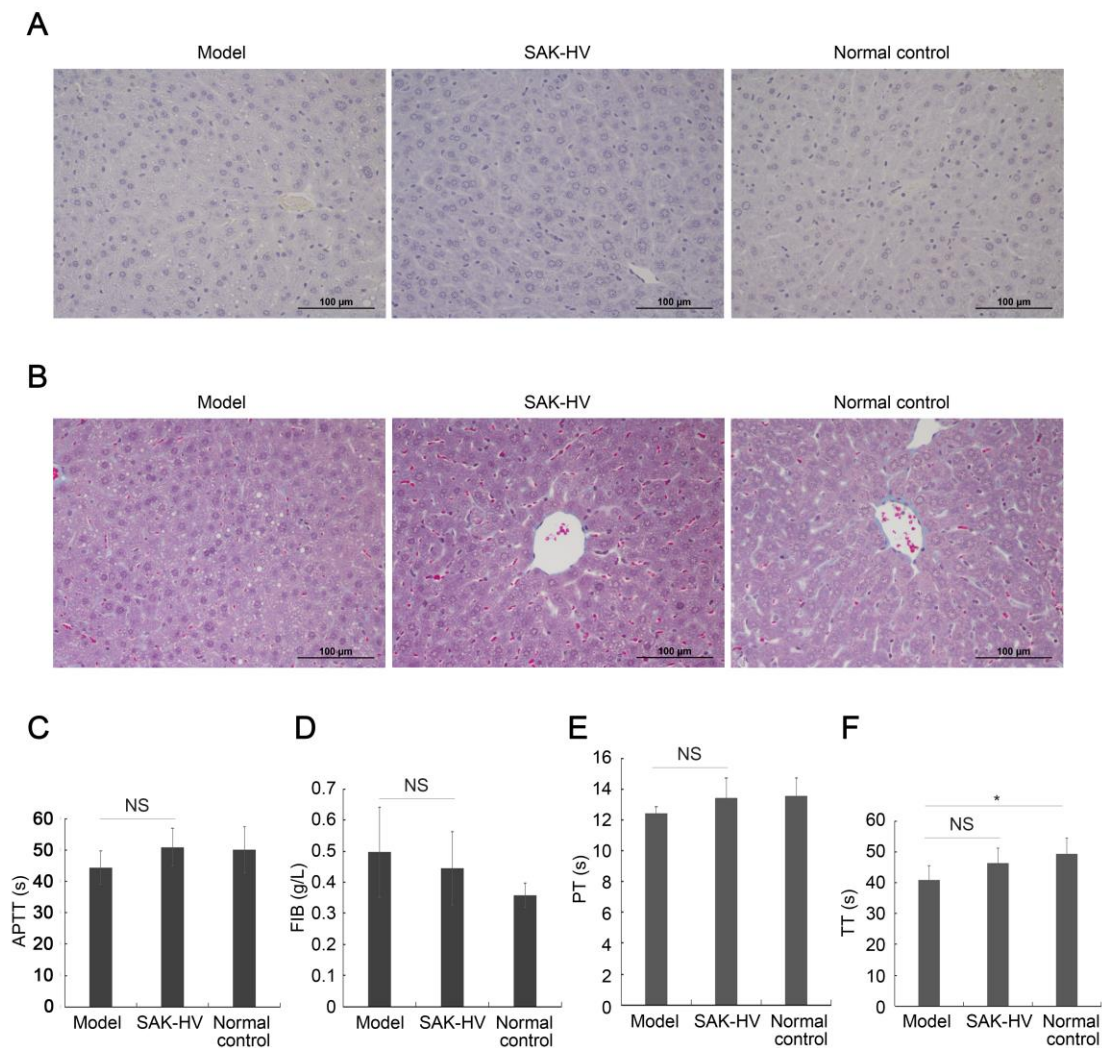


Figure S2. The liver pathological examination and the blood coagulation function detection. (A) The TUNEL detection indicated that SAK-HV treatment caused no apoptosis in liver (n=4). (B) The Masson trichrome staining showed that SAK-HV treatment caused no fibrosis in liver (n=4). (C) Although SAK-HV caused no significant changes of coagulation function in *ApoE*^{-/-} mice, it mildly improved these indexes to be similar to these of the normal group (n=6).

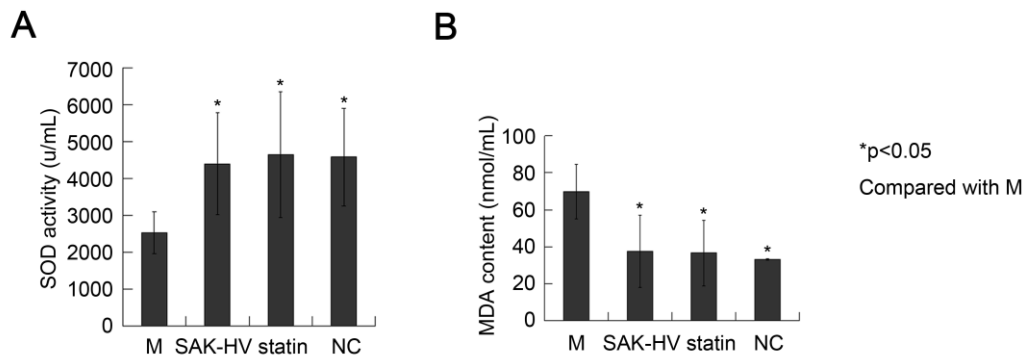


Figure S3. The comparison of the anti-oxidative stress effect between SAK-HV injection (0.125mg/kg) and oral administration of atorvastatin (100mg/kg). (A and B) The anti-oxidative stress effect of SAK-HV was similar to that of the atorvastatin (n=8). Abbreviations: M, model; NC, normal control; SOD, Superoxide Dismutase; MDA, Maleic Dialdehyde.

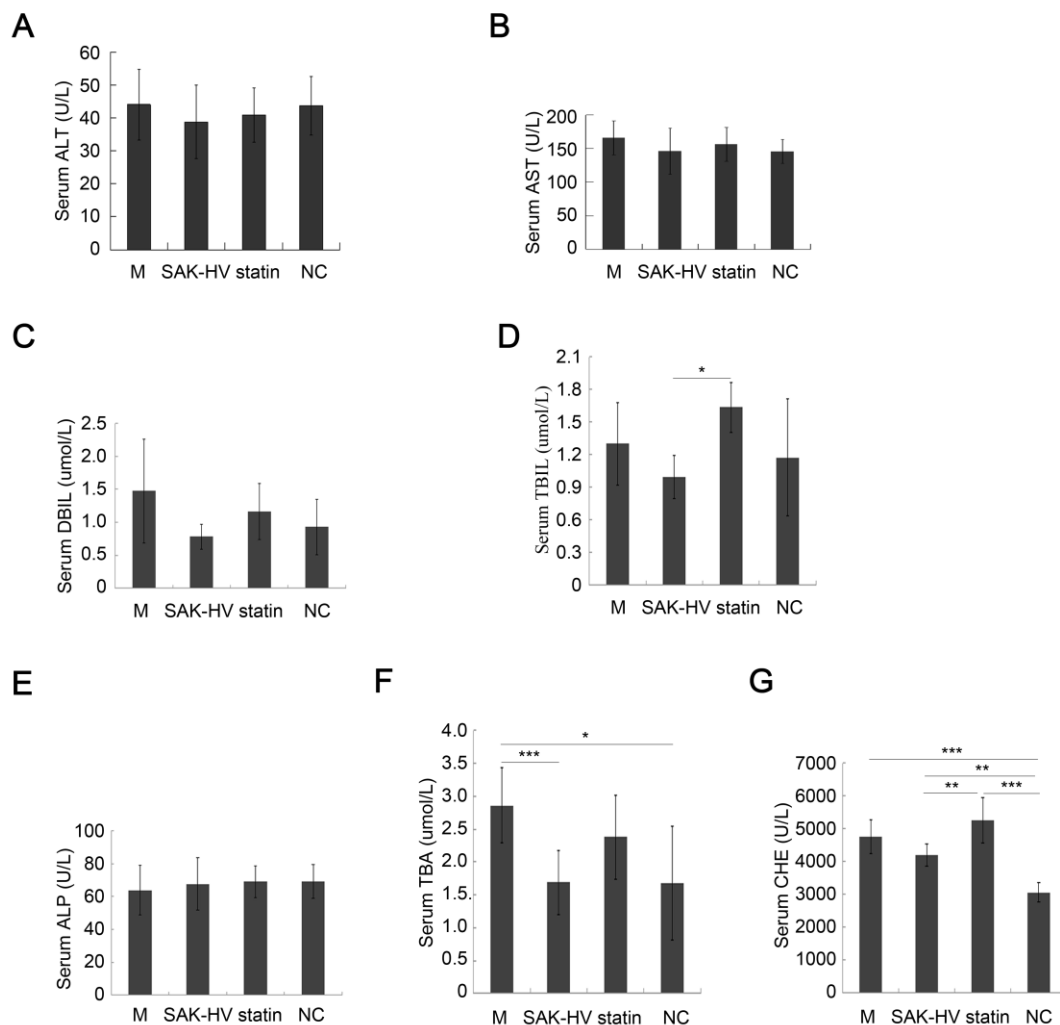


Figure S4. The comparison of the liver function between model, SAK-HV, atorvastatin and normal groups. The serum levels of (A) ALT, (B) AST, (C) DBIL, (D) TBIL, (E) ALP, (F) TBA and (G) CHE were detected to check the liver function (n=8 for A-G). SAK-HV treatment improved the liver function to be similar to that of normal group, except for the serum level of CHE. However, it was significantly better than that of atorvastatin group. Abbreviations: ALT, alanine aminotransferase; AST, aspartate aminotransferase; DBIL, direct bilirubin; TBIL, total bilirubin; ALP, alkaline phosphatase; TBA, Total bile acids; CHE, cholinesterase.

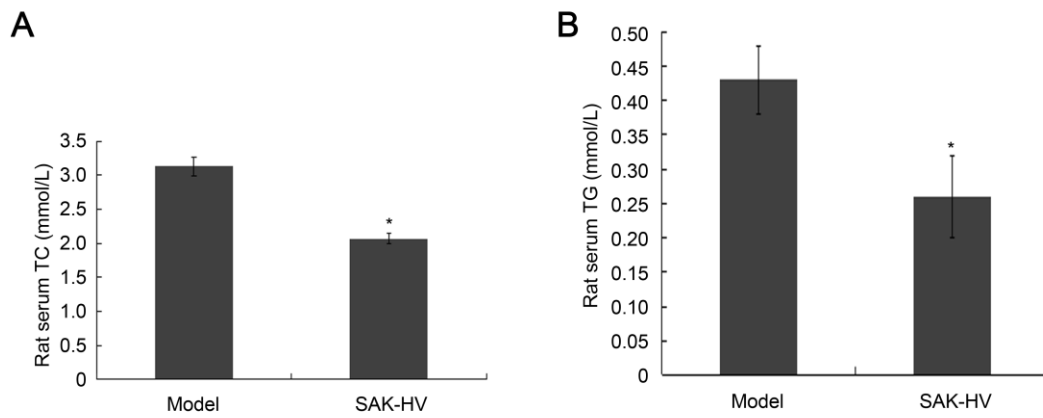


Figure S5. The lipid-lowering effect of SAK-HV on high-fat-fed rats. (A and B) SAK-HV effectively lowered the serum triglyceride and serum total cholesterol in high-fat-fed rats. Abbreviation: TG, triglyceride; TC total cholesterol.

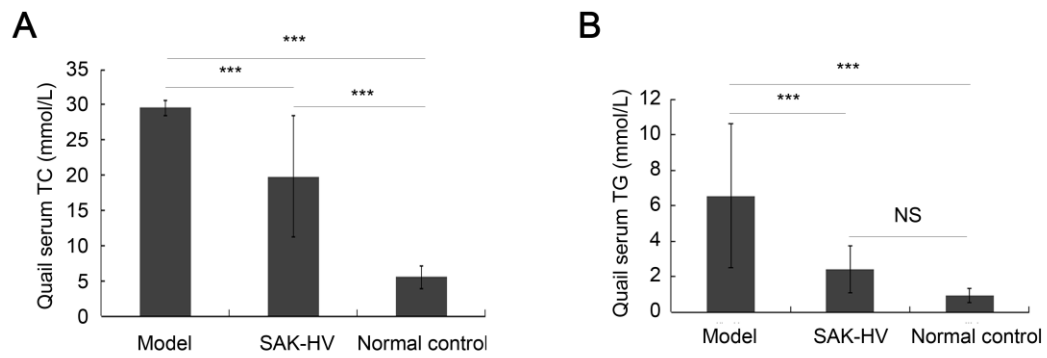


Figure S6. The lipid-lowering effect of SAK-HV on high-fat-fed quails. (A and B) SAK-HV effectively lowered the serum triglyceride and serum total cholesterol in high-fat-fed quails.

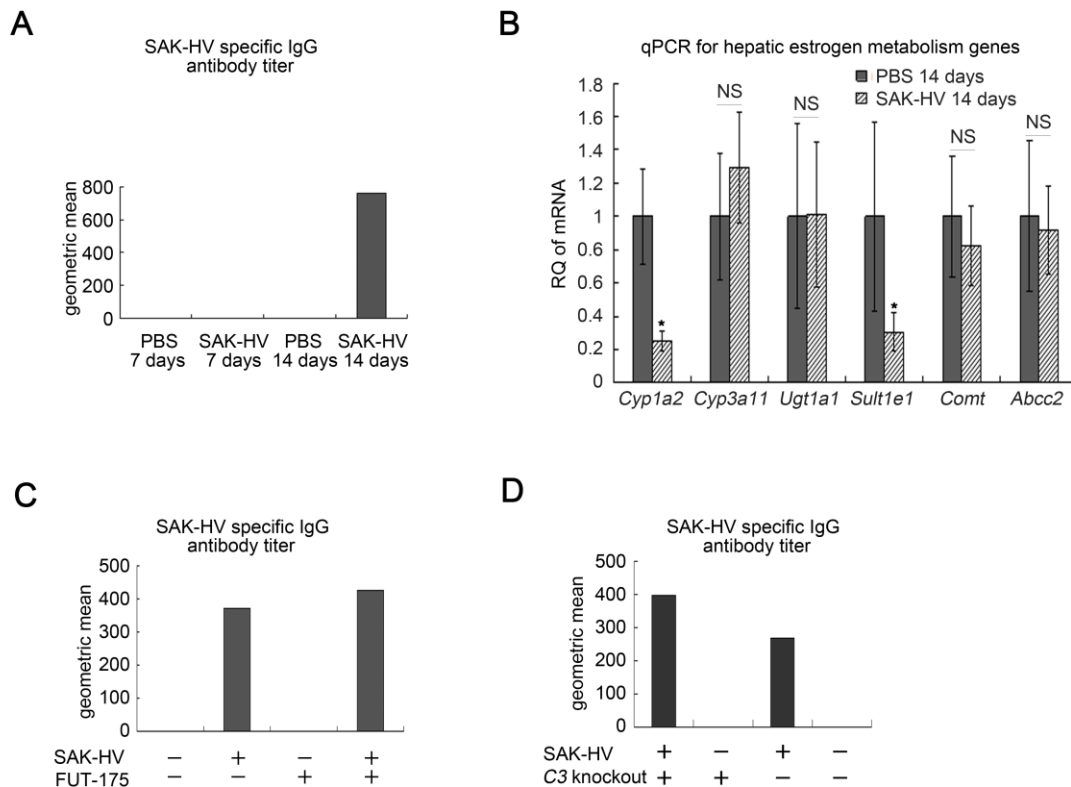


Figure S7. The titers of SAK-HV-specific IgG in serum after SAK-HV treatment.

(A) SAK-HV-specific IgG in serum had not been generated on the 7th day, but its antibody titer to SAK-HV reached $10^{2.88}$ on the 14th day. (B) The effect of SAK-HV treatment on the transcription levels of genes involved in estrogen metabolism and excretion in liver (n=6). (C) The titers of SAK-HV-specific IgG in serum reached $10^{2.63}$ and $10^{2.57}$ on the 14th day in the FUT-175+SAK-HV and SAK-HV group, respectively. (D) The titers of SAK-HV-specific IgG in serum reached $10^{2.6}$ and $10^{2.43}$ on the 14th day in the SAK-HV $C3^{-/-}$ and SAK-HV $C3^{+/+}$ groups, respectively. Abbreviation: *Cyp1a2*, cytochrome P450 family 1 subfamily A member 2; *Cyp3a11*, cytochrome P450 family 3 subfamily A member 11; *Ugt1a1*, UDP Glucuronosyltransferase Family 1 Member A1; *Sult1e1*, sulfotransferase family 1E member 1; *Comt*, catechol-O-methyltransferase; *Abcc2*, ATP Binding Cassette Subfamily C Member 2.

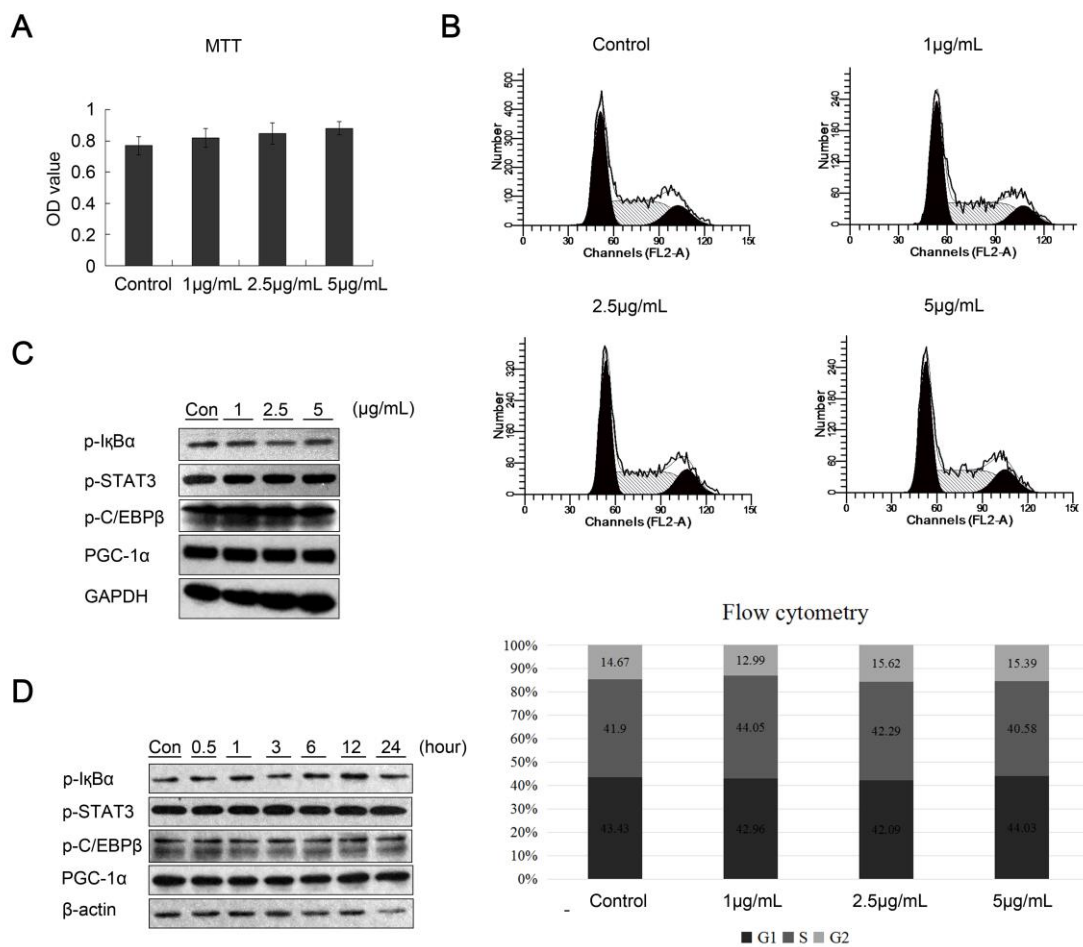


Figure S8. The effect of SAK-HV stimulus on murine embryonic hepatocyte BNL-CL2 cells *in vitro*. (A,B) The results of MTT assay and flow cytometry showed that the direct stimulus of SAK-HV at all the concentrations to BNL-CL2 for 24 h caused no proliferation effects, and led to no changes in the cell cycle. (C) The stimulus of SAK-HV at all concentrations to BNL-CL2 for 24 h did not activate IκBα and the STAT3-C/EBPβ-PGC-1α pathway. (D) SAK-HV stimulus (5µg/mL) did not activate IκBα and the STAT3-C/EBPβ-PGC-1α pathway at any time point. SAK-HV at a concentration gradient was used to stimulate BNL-CL2 cells for 24 h. Then, 5µg/mL SAK-HV was used to stimulate BNL-CL2 cells for different time. The PBS-treated BNL-CL2 cells were used as the blank control for both assays. Abbreviation: PGC-1α, PPARγ coactivator-1 α.

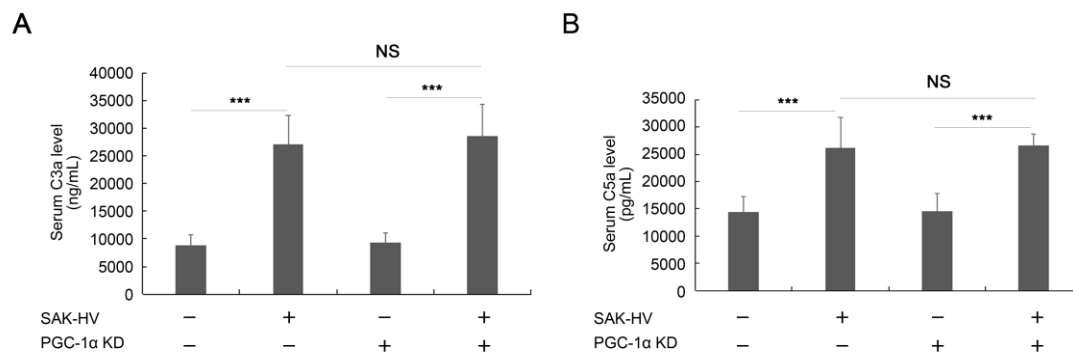


Figure S9. The effect of PPAR α inhibition caused by PGC-1 α Knockdown on SAK-HV-induced complement activation. (A,B) PPAR α inhibition caused by PGC-1 α Knockdown led to no significant changes in serum levels of C3a and C5a (n=7). Abbreviation: KD, Knockdown.

Supplementary Tables

Table S1

The primers for qPCR analysis.

Genes	primers	Sequences
<i>Ppara</i>	Forward	5' GGCTCGGAGGGCTCTGTCATC 3'
	Reverse	5' ACATGCACTGGCAGCAGTGGA 3'
<i>C1q</i>	Forward	5' GCACTCCAGGGATAAAGGGG 3'
	Reverse	5' AGGCGACTTTCTGTGTAGCC 3'
<i>Nr5a2</i>	Forward	5' CTGATACTGGAACTTTTGAA 3'
	Reverse	5' CTTCATTTGGTCATCAACCTT 3'
<i>Hsd3b2</i>	Forward	5' TCCAGTTGTTGGTGCAAGAGG 3'
	Reverse	5' TCCTCAGGTACTGGGTGTCA 3'
<i>Cpt1a</i>	Forward	5' CCAGGCTACAGTGGGACATT 3'
	Reverse	5' GAACTTGCCCATGTCCTTGT 3'
<i>Ldlr</i>	Forward	5' GGGAACATTTTCGGGGTCTGT 3'
	Reverse	5' AGTCTTCTGCTGCAACTCCG 3'
<i>Cyp19a1</i>	Forward	5' CATTATCAGCAAGTCCTCAAGC 3'
	Reverse	5' GAGGGTCAACACATCCACG 3'
<i>Cyp7a1</i>	Forward	5' AGCAACTAAACAACCTGCCAGTACTA 3'
	Reverse	5' GTCCGGATATTCAAGGATGCA 3'
<i>Abcg8</i>	Forward	5' AATGTCATCCTGGATGTCGTCTC 3'
	Reverse	5' CCAGCTCATAGTACAGCATTGACC 3'

<i>Abcg5</i>	Forward	5' TCAATGAGTTTTACGGCCTGAA 3'
	Reverse	5' GCACATCGGGTGATTTAGCA 3'
<i>Acot3</i>	Forward	5' TGGAATTGGAAGTGGCCTTCTGGA 3'
	Reverse	5' AACCTGTTACCTGAGGGTGA 3'
<i>Acot4</i>	Forward	5' AACATCGATGATGCCTGGA 3'
	Reverse	5' GTCACTTCATGGCTCCCG 3'
<i>Cyp1a2</i>	Forward	5' AAGACAATGGCGGTCTCATC 3'
	Reverse	5' GACGGTCAGAAAGCCGTGGT 3'
<i>Cyp3a11</i>	Forward	5' GACAAACAAGCAGGGATGGAC 3'
	Reverse	5' CCAAGCTGATTGCTAGGAGCA 3'
<i>Sult1e1</i>	Forward	5' GGAACGCCAAAGATGTCGCCG 3'
	Reverse	5' ACCATACGGA 3'
<i>Comt</i>	Forward	5' ACACACTGGACATGGTCTTCCT 3'
	Reverse	5' ATCACGTTGTCAGCCAGTAGCA 3'
<i>Abcc2</i>	Forward	5' GCTGAGATCGGAGAGAAGGGTA 3'
	Reverse	5' CACTTGGGGAAGGAAGTGAA 3'
<i>Ugt1a1</i>	Forward	5' TGA 3'
	Reverse	5' GGAATAA 3'
<i>Gapdh</i>	Forward	5' GAGTCAACGGATTTGGTCGT 3'
	Reverse	5' TTGATTTTGGAGGGATCTCG 3'

Table S2

The SAK-HV-triggered differentially expressed genes.

Please see file “Table S2.xls”.

The mRNA samples of mice liver (7 from SAK-HV 0.125mg/kg group and 5 from control group) were analyzed for gene expression profiling on the illumina WG-6V2 transcriptome chips. The differentially expressed genes listed in the table were identified by the Rank Product method (RankProd).

Table S3

GO enrichment of biological process for upregulated genes.

category	GOID	Term	P-value
biological process	GO:0002376	Immune system process	4.52E-14
biological process	GO:0006952	Defense response	7.07E-10
biological process	GO:0002682	Regulation of immune system process	1.05E-09
biological process	GO:0008152	Metabolic process	1.05E-09
biological process	GO:0070887	Cellular response to chemical stimulus	1.05E-09
biological process	GO:0048523	Negative regulation of cellular process	1.30E-09
biological process	GO:0048518	Positive regulation of biological process	1.62E-09
biological process	GO:0048519	Negative regulation of biological process	1.62E-09
biological process	GO:0044710	Single-organism metabolic process	3.55E-09
biological process	GO:0006950	Response to stress	3.55E-09
biological process	GO:0048522	Positive regulation of cellular process	5.72E-09
biological process	GO:0042221	Response to chemical stimulus	5.97E-09
biological process	GO:0045087	Innate immune response	9.75E-09
biological process	GO:0006955	Immune response	2.41E-08
biological process	GO:0071704	Organic substance metabolic process	7.34E-08
biological process	GO:0019886	Antigen processing and presentation of exogenous peptide antigen via MHC class II	7.34E-08
biological process	GO:0002684	Positive regulation of immune system process	1.44E-07

biological process	GO:0045321	Leukocyte activation	1.45E-07
biological process	GO:0001775	Cell activation	1.69E-07
biological process	GO:0002495	Antigen processing and presentation of peptide antigen via MHC class II	1.91E-07
biological process	GO:0008202	Steroid metabolic process	3.25E-07
biological process	GO:0016064	Immunoglobulin mediated immune response	3.25E-07
biological process	GO:0044238	Primary metabolic process	3.99E-07
biological process	GO:0019724	B cell mediated immunity	3.99E-07
biological process	GO:0034097	Response to cytokine stimulus	5.43E-07
biological process	GO:0002250	Adaptive immune response	5.43E-07
biological process	GO:0002504	Antigen processing and presentation of peptide or Polysaccharide antigen via MHC class II	5.98E-07
biological process	GO:0010033	Response to organic substance	6.03E-07
biological process	GO:0019882	Antigen processing and presentation	6.03E-07
biological process	GO:0070663	Regulation of leukocyte proliferation	9.19E-07
biological process	GO:0002478	Antigen processing and presentation of exogenous peptide antigen	1.17E-06
biological process	GO:0002460	Adaptive immune response based on somatic recombination of immune receptors built from immunoglobulin superfamily domains	1.23E-06

biological process	GO:0048513	Organ development	1.29E-06
biological process	GO:0050867	Positive regulation of cell activation	1.94E-06
biological process	GO:0048002	Antigen processing and presentation of peptide antigen	2.10E-06
biological process	GO:0046649	Lymphocyte activation	2.43E-06
biological process	GO:0030097	Hemopoiesis	2.88E-06
biological process	GO:0070661	Leukocyte proliferation	2.88E-06
biological process	GO:0002455	Humoral immune response mediated by circulating immunoglobulin	2.88E-06
biological process	GO:0048534	Hematopoietic or lymphoid organ development	2.88E-06

All the P-values from the hypergeometric test were Benjamini-Hochberg corrected.

Table S4

KEGG pathway enrichment for upregulated genes.

category	KEGG ID	KEGG pathway name	P-value
KEGG pathway	5322	Systemic lupus erythematosus	1.72E-11
KEGG pathway	5150	Staphylococcus aureus infection	9.53E-07
KEGG pathway	5020	Prion diseases	1.55E-06
KEGG pathway	100	Steroid biosynthesis	3.21E-06
KEGG pathway	4612	Antigen processing and presentation	1.67E-05
KEGG pathway	5140	Leishmaniasis	8.68E-05
KEGG pathway	4610	Complement and coagulation cascades	1.00E-04
KEGG pathway	4145	Phagosome	2.00E-04
KEGG pathway	5310	Asthma	2.00E-04
KEGG pathway	3320	PPAR signaling pathway	2.00E-04
KEGG pathway	4380	Osteoclast differentiation	6.00E-04
KEGG pathway	4920	Adipocytokine signaling pathway	4.20E-03
KEGG pathway	5145	Toxoplasmosis	5.20E-03
KEGG pathway	140	Steroid hormone biosynthesis	5.40E-03
KEGG pathway	5416	Viral myocarditis	8.40E-03
KEGG pathway	4672	Intestinal immune network for IgA production	2.00E-02
KEGG pathway	5332	Graft-versus-host disease	2.27E-02

KEGG pathway	5330	Allograft rejection	2.33E-02
KEGG pathway	4520	Adherens junction	2.43E-02
KEGG pathway	5323	Rheumatoid arthritis	3.23E-02
KEGG pathway	4940	Type I diabetes mellitus	3.36E-02
KEGG pathway	4512	ECM-receptor interaction	4.20E-02
KEGG pathway	260	Glycine, serine and threonine metabolism	4.76E-02
KEGG pathway	5320	Autoimmune thyroid disease	4.76E-02

All the P-values from the hypergeometric test were Benjamini-Hochberg corrected.

Table S5

The most relevant modules of cholesterol or triglyceride metabolism identified by WGCNA algorithm for SAK-HV group.

Please see file “Table S5.xls”.

The lipid metabolism related modules were obtained by WGCNA algorithm for SAK-HV group with the correlation coefficient of 0.7 as the cutoff. The genes were listed in descending order of the intramodular connectivity in their own module.

Table S6

GO enrichment of biological process for cyan module.

category	GO ID	Term	P-value
biological process	GO:0044238	Primary metabolic process	4.66E-09
biological process	GO:0071704	Organic substance metabolic process	1.61E-08
biological process	GO:0044710	Single-organism metabolic process	8.36E-08
biological process	GO:0008152	Metabolic process	8.36E-08
biological process	GO:0044237	Cellular metabolic process	3.62E-07
biological process	GO:0006807	Nitrogen compound metabolic process	7.14E-05
biological process	GO:0034641	Cellular nitrogen compound metabolic process	3.00E-04
biological process	GO:1901360	Organic cyclic compound metabolic process	4.00E-04
biological process	GO:0043170	Macromolecule metabolic process	5.00E-04
biological process	GO:0044260	Cellular macromolecule metabolic process	1.00E-03
biological process	GO:1901576	Organic substance biosynthetic process	1.00E-03
biological process	GO:0006725	Cellular aromatic compound metabolic process	1.60E-03
biological process	GO:0009058	Biosynthetic process	1.60E-03
biological process	GO:0080090	Regulation of primary metabolic process	1.60E-03
biological process	GO:0046483	Heterocycle metabolic process	2.20E-03

biological process	GO:0044249	Cellular biosynthetic process	3.30E-03
biological process	GO:0006139	Nucleobase-containing compound metabolic process	3.80E-03
biological process	GO:0032330	Regulation of chondrocyte differentiation	3.80E-03
biological process	GO:0019538	Protein metabolic process	3.80E-03
biological process	GO:0044281	Small molecule metabolic process	4.70E-03
biological process	GO:0042254	Ribosome biogenesis	6.20E-03
biological process	GO:0048522	Positive regulation of cellular process	6.20E-03
biological process	GO:0061035	Regulation of cartilage development	9.40E-03
biological process	GO:0060414	Aorta smooth muscle tissue morphogenesis	9.40E-03
biological process	GO:0019222	Regulation of metabolic process	9.40E-03
biological process	GO:0044267	Cellular protein metabolic process	9.40E-03
biological process	GO:0071840	Cellular component organization or biogenesis	9.40E-03
biological process	GO:0031323	Regulation of cellular metabolic process	9.40E-03
biological process	GO:0048518	Positive regulation of biological process	9.40E-03
biological process	GO:0044085	Cellular component biogenesis	1.32E-02
biological process	GO:0010467	Gene expression	1.32E-02
biological process	GO:0006259	DNA metabolic process	1.65E-02
biological process	GO:1901135	Carbohydrate derivative metabolic process	1.65E-02

biological process	GO:0009987	Cellular process	1.94E-02
biological process	GO:0051919	Positive regulation of fibrinolysis	1.94E-02
biological process	GO:0019637	Organophosphate metabolic process	2.27E-02
biological process	GO:0009059	Macromolecule biosynthetic process	2.51E-02
biological process	GO:0006796	Phosphate-containing compound metabolic process	2.51E-02
biological process	GO:1901564	Organonitrogen compound metabolic process	2.79E-02
biological process	GO:0042278	Purine nucleoside metabolic process	3.06E-02

The cyan module was the most relevant module of cholesterol metabolism identified by WGCNA algorithm for SAK-HV group. All the P-values from the hypergeometric test were Benjamini-Hochberg corrected.

Table S7

KEGG pathway enrichment for turquoise module.

category	GOID	Term	P-value
KEGG pathway	1100	Metabolic pathways	4.64E-11
KEGG pathway	3040	Spliceosome	6.02E-05
KEGG pathway	4146	Peroxisome	4.00E-04
KEGG pathway	450	Selenocompound metabolism	8.00E-04
KEGG pathway	250	Alanine, aspartate and glutamate metabolism	1.50E-03
KEGG pathway	3013	RNA transport	2.10E-03
KEGG pathway	3060	Protein export	1.21E-02
KEGG pathway	71	Fatty acid metabolism	1.21E-02
KEGG pathway	20	Citrate cycle (TCA cycle)	2.33E-02
KEGG pathway	480	Glutathione metabolism	2.33E-02
KEGG pathway	4141	Protein processing in endoplasmic reticulum	3.00E-02
KEGG pathway	270	Cysteine and methionine metabolism	3.40E-02
KEGG pathway	4120	Ubiquitin mediated proteolysis	3.74E-02
KEGG pathway	982	Drug metabolism - cytochrome P450	3.74E-02
KEGG pathway	3320	PPAR signaling pathway	3.88E-02
KEGG pathway	520	Amino sugar and nucleotide sugar	3.88E-02

metabolism			
KEGG pathway	640	Propanoate metabolism	4.34E-02
KEGG pathway	4962	Vasopressin-regulated water reabsorption	4.75E-02
KEGG pathway	280	Valine, leucine and isoleucine degradation	4.75E-02
KEGG pathway	230	Purine metabolism	4.75E-02

The turquoise was the most relevant module of triglyceride metabolism identified by WGCNA algorithm for SAK-HV group. All the P-values from the hypergeometric test were Benjamini-Hochberg corrected.

Table S8

136 up-regulated genes in turquoise module.

Please see file "Table S8.xls".

The upregulated genes in turquoise module were obtained by determining the intersection of the upregulated genes and genes of turquoise based on the hypothesis that the important hub genes are usually differential expression genes.

Table S9

Wikipathway pathway enrichment for up-regulated genes in turquoise module.

category	Gene Set ID	Gene Set Name	P-value
Wikipathways pathway	WP103	Cholesterol Biosynthesis	1.62E-05
Wikipathways pathway	WP447	Adipogenesis	3.52E-05
Wikipathways pathway	WP1268	Diurnally regulated genes with circadian orthologs	4.00E-04
Wikipathways pathway	WP2316	PPAR signaling pathway	4.00E-04
Wikipathways pathway	WP544	Circadian Exercise	6.20E-03
Wikipathways pathway	WP1267	Senescence and Autophagy	7.00E-03
Wikipathways pathway	WP298	G13 Signaling Pathway	3.72E-02
Wikipathways pathway	WP193	Signaling of Hepatocyte Growth Factor Receptor	3.72E-02
Wikipathways pathway	WP1249	EPO Receptor Signaling	3.72E-02
Wikipathways pathway	WP1259	Retinol metabolism	3.84E-02
Wikipathways pathway	WP157	Glycolysis and Gluconeogenesis	3.84E-02
Wikipathways pathway	WP297	IL-7 Signaling Pathway	3.84E-02
Wikipathways pathway	WP387	IL-6 signaling Pathway	3.84E-02

The upregulated genes in turquoise module were obtained by determining the intersection of the upregulated genes and genes of turquoise based on the hypothesis

that the important hub genes are usually differential expression genes. All the P-values from the hypergeometric test were Benjamini-Hochberg corrected.

Supplementary methods

Animal experiments design.

For the pharmacodynamic evaluation of SAK-HV, total 40 male *ApoE*^{-/-} mice were randomly divided into model group (PBS i.v.; n=8) and 4 SAK-HV groups, including 0.0625mg/kg group, 0.125mg/kg group, 0.25mg/kg group and 0.5mg/kg group (SAK-HV i.v.; n=8 separately). The male wild-type C57BL/6J mice with the same genetic background were used as blank control group (n=8). For each group, mice were sacrificed on the 14th day of the treatment period. In addition, the 48 male *ApoE*^{-/-} mice were randomly divided into model group (PBS i.v.; n=12) and 3 SAK-HV groups, including SAK-HV 7 days group, SAK-HV 10 days group, and SAK-HV 14 days group (SAK-HV 0.125mg/kg i.v.; n=12 separately;), for which mice were sacrificed on the 7th, 10th and 14th day of the treatment period, separately. The male wild-type C57BL/6J mice with the same genetic background were used as blank control group (n=8).

In comparison of the lipid-lowering effects between SAK-HV and atorvastatin, the male *ApoE*^{-/-} mice were randomly divided into 3 groups: SAK-HV group (SAK-HV 0.125mg/kg i.v.; n=8), model group (PBS i.v.; n=8), and statin group (atorvastatin 100mg/kg p.o.; Pfizer, New York, NY; n=8) (29), separately. In addition, the male wild-type C57BL/6J mice with the same genetic background were used for normal control group (n=8). All the mice were sacrificed on the 14th day of the treatment period.

In the experiment for SAK-HV-triggered biological disturbances detection, the male *ApoE*^{-/-} mice were randomly divided into SAK-HV 7 days group (SAK-HV 0.125mg/kg i.v.; n=6), SAK-HV 14 days group (SAK-HV 0.125mg/kg i.v.; n=6), PBS 7 days group (PBS i.v.; n=6), and PBS 14 days group (PBS i.v.; n=6), separately. The mice of 7 days group and 14s day group were sacrificed on the 7th and 14th day of the treatment period, separately.

For all the experiments below, the mice were sacrificed on the 14th day of the treatment period.

In the experiment of STAT3 phosphorylation inhibition, the male *ApoE*^{-/-} mice were randomly divided into 4 groups: SAK-HV group (SAK-HV 0.125mg/kg i.v.; n=8), STATTIC group (STATTIC 1µg/kg i.p.; Selleck Chemicals, Houston, TX, USA; n=8), SAK-HV+STATTIC group (SAK-HV 0.125mg/kg i.v., STATTIC 1µg/kg i.p.; n=8), and model group (PBS i.v. n=8) .

In the experiment of complement activation inhibition, the male *ApoE*^{-/-} mice were randomly divided into 4 groups: SAK-HV group (SAK-HV 0.125mg/kg i.v.; n=8), FUT-175 group (FUT-175 10mg/kg i.p.; Selleck Chemicals, Houston, TX, USA; n=8), SAK-HV+FUT-175 group (SAK-HV 0.125mg/kg i.v., FUT-175 10mg/kg i.p.; n=8), and model group (PBS i.v. n=8).

In the experiment of *C3* knockout, the male *C3*^{-/-} mice were randomly divided into *C3* knockout SAK-HV group (SAK-HV 0.125mg/kg i.v.; n=6) and *C3* knockout group (PBS i.v.; n=6); the male *C3*^{+/+} mice with the same genetic background were randomly divided into SAK-HV group (SAK-HV 0.125mg/kg i.v.; n=6) and control group (PBS i.v.; n=6).

In the experiment of PGC-1 α knockdown, the male PGC-1 α knockdown *ApoE*^{-/-} mice were randomly divided into PGC-1 α knockdown SAK-HV group (SAK-HV 0.125mg/kg i.v.; n=7) and PGC-1 α knockdown control group (PBS i.v.; n=7); the male *ApoE*^{-/-} mice with the same genetic background were randomly divided into SAK-HV group (SAK-HV 0.125mg/kg i.v.; n=7) and control group (PBS i.v. n=7).

In the experiment of estrogen inhibition, the male *ApoE*^{-/-} mice were randomly divided into SAK-HV group (SAK-HV 0.125mg/kg i.v. n=10), letrozole group (letrozole 20 μ g/day per mouse i.s.; Selleck Chemicals, Houston, TX, USA; n=10), SAK-HV+letrozole group (SAK-HV 0.125mg/kg i.v., letrozole 20 μ g/day per mouse i.s.; n=8) and model group (PBS i.v.; n=10), separately.

Supplementary information

Introduction about SAK-HV.

SAK-HV is a recombinant fusion protein constructed by our lab. It composed of a staphylokinase variant, tripeptide of arg-gly-asp (RGD), and a segment of 12 amino acid residues at the C-terminus of hirudin (20). This recombinant protein has multiple functions, including thrombolysis, anti-coagulation, and the inhibition of platelet aggregation (20). We designed this protein for the purpose of treating atherosclerosis.

1) The source, purity, physicochemical property, formulation for administration and pharmacokinetic characteristics of SAK-HV.

SAK-HV was expressed in *E.coli* system. The molecular weight of SAK-HV is 17.1 kDa, and its isoelectric point is 5.3. After the purification, the HPLC (High Performance Liquid Chromatogram) detection result showed that the protein purity of SAK-HV exceeds 95%. SAK-HV is dissolved in PBS buffer (pH7.3), then it can be stored at 4°C for one year to keep stability.

We analyzed the tissue distribution of total radioactivity and radioactivity of acid deposition at different points in time after ¹²⁵I-SAK-HV administration in BALB/C mice via tail vein in pharmacokinetic study. The results showed that the largest concentrations of ¹²⁵I-SAK-HV accumulated in the urine and kidney, indicating a rapid degradation of SAK-HV in BALB/C mice after intravenous injection. We further analyzed the half-time of SAK-HV via ¹²⁵I-SAK-HV administration in Wistar

rats, The results indicated that its serum half-life in rats was about 60 min.

2) The pharmacodynamics characteristics of SAK-HV

Pharmacodynamic evaluation of SAK-HV indicated that the effective dosages of SAK-HV to achieve a lipid-reducing effect for *ApoE*^{-/-} mice ranged from 0.0625 to 0.5 mg/kg, and the optimal dosage was 0.125 mg/kg. It was injected into the mice via tail vein every other day for 7 times within the 14-day treatment cycle. Besides that, SAK-HV significantly decreases the levels of both inflammatory cytokines and oxidative stress in serum, and effectively blocks the development of atherosclerosis in high-fat-fed *ApoE*^{-/-} mice, rats and quails (unpublished data).

3) The acute toxicity of SAK-HV

We first carry out the preliminary acute toxicity test of SAK-HV on mice. All the mice were injected with SAK-HV at a maximum dose of 600mg/kg via tail vein. After 2-week observation period, all mice were survival, and no obvious pathological changes were found in any organs of mice.

We then formally carry out the acute toxicity test of SAK-HV on SD rats, following the GLP (Good Laboratory Practice for Non-clinical Laboratory Studies) standards.

All the rats were injected with SAK-HV at a maximum dose of 572mg/kg via tail vein, and no obvious systemic toxicity were observed during the 2-week observation period.

All rats were survival after 2-week observation period, and no obvious pathological

changes were found in any organs of rats. This acute toxicity of SAK-HV on rats was completed in the NBCDSER (National Beijing Center for Drug Safety Evaluation and Research), An AAALAC Full Accreditation institution (#1351).